Research article

Journal of MASS SPECTROMETRY

Received: 25 March 2014 Revised: 2 August 2014 Accepted: 5 August 2014 Published online in Wiley Online Library

(wileyonlinelibrary.com) DOI 10.1002/jms.3461

Structure elucidation of phototransformation products of unapproved analogs of the erectile dysfunction drug sildenafil in artificial freshwater with UPLC-Q Exactive-MS

Jaume Aceña,[a] Sandra Pérez,[a]* Piero Gardinali,[b] José Luis Abad,[c] Peter Eichhorn,[a] Nubia Heuett[b] and Damià Barceló[a,d]

In this study, four unapproved analogues of Sildenafil (SDF) were photodegraded under synthetic sunlight in artificial freshwater. Homosildenafil (H-SDF), hydroxyhomo-sildenafil (HH-SDF), norneosildenafil (NR-SDF) and thiosildenafil (T-SDF) were selected because they are frequently detected as adulterants in natural herbal products. Using UPLC-Orbitrap (Q Exactive)-MS, six photoproducts common to H-SDF, HH-SDF and T-SDF and nine unique transformation products of different molecular weights were identified based on their high-resolution (+)ESI product ion spectra. Mass spectral analysis of deuterated H-SDF, labeled on the N-ethyl group, allowed to gain mechanistic insight into the fragmentation pathway of the substituted piperazine ring and to support the postulated photoproduct structures. The mass spectral fragmentation confirmed the stepwise destruction of the piperazine ring eventually producing a sulfonic acid derivative ($C_{17}H_{20}N_4O_5S$: 392.1151 Da). In contrast, the photodegradation of NR-SDF, which lacks a piperazine ring in its structure, formed only two prominent photoproducts originating from *N,N*-dealkylation of the sulfonamide followed by hydrolysis. The current work constitutes the first study on the photodegradation of analogs of erectile dysfunction drugs and the first detection of two transformation products (*m/z* 449 and 489) in environmental samples. Copyright © 2014 John Wiley & Sons, Ltd.

Additional supporting information may be found in the online version of this article at the publisher's web site.

Keywords: analogs of erectile dysfunction drugs; photolysis; transformation products; high-resolution mass spectrometry

Introduction

In the European Union three drugs are approved for the treatment of erectile dysfunction, namely sildenafil citrate, vardenafil hydrochloride (Levitra™, Bayer) and tadalafil (Cialis™, Elli Lilly). These phosphodiesterase type V (PDE-5) inhibitors act on the smooth muscle cells lining blood vessels, especially in the corpus cavernosum of the penis. While these approved lifestyle drugs are in principle only available exclusively by medical prescription, growing evidence points to the undeclared presence of these PDE-5 inhibitors and structurally closely related analogs in herbal medicines and dietary supplements for erectile dysfunction[1] Many cases of adulterated products have been reported from East and Southeast Asian countries.[2,3] Consumers in other parts of the world may also be exposed unknowingly to such adulterated products that they can readily purchase through internet portals. Besides the unintentional exposure to any of the three aforementioned erectile dysfunction drugs, human health risks arise particularly from the presence of unapproved analogs containing minor structural modifications because they have not undergone extensive safety testing. Since the first detection of homosildenafil (H-SDF) in 2003 in herbal formulations,[4] a series of derivatives of SDF, vardenafil and tadalafil have been identified in adulterated products.[1,5,6] As the chemical structures of many of them are claimed in patents, they can be expected to exert pharmacological effects in humans, but toxicological safety profiles, as available for the three approved compounds, which underwent comprehensive preclinical testing and subsequently clinical studies, are not released for any of the derivatives.

Regarding the first-in-class PDE-5 inhibitor SDF, its synthetic analogs that have been identified include the so-called homo-SDF (H-SDF), homohydroxy-SDF (HH-SDF), thio-SDF (T-SDF) and norneo-SDF (NR-SDF) (for structures see Scheme 1).[7] As little as is known about the pharmacodynamics of the adulterants that have been tracked down in a number of dietary supplements,[8–12] their disposition in the human body is expectedly unknown. Ultimately, however, all these exogenous substances are subject to excretory

* Correspondence to: Sandra Pérez, IDAEA-CSIC, Water and Soil Quality Research Group, Jordi Girona 18-26, Barcelona 08034, Spain. E-mail: spsqam@idaea.csic.es

a Water and Soil Quality Research Group, IDAEA-CSIC, c/Jordi Girona 18-26, 08034, Barcelona, Spain

b Florida International University, 11200 SW 8th Street, Miami, Florida, 33199-0001, USA

c IQAC-CSICDepartment of Biomedicinal ChemistryJordi Girona 18-26, 08034, Barcelona, Spain

d Catalan Institute of Water Research, ICRA Catalan Institute for Water Research-ICRA, C/Emili Grahit, 101, Edifici H_2O, Parc Científic i Tecnològic de la Universitat de Girona, E-17003, Girona, Spain

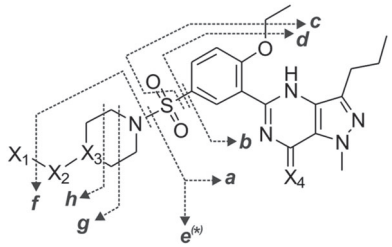

	Substituent				Fragmentation								
Compound	X_1	X_2	X_3	X_4	*a*	*b*	*c*	*d*	*e*	*e**	*f*	g	h
SDF	H	CH_2	N	O	377	311	299	283	99	100	-	70	58
H-SDF	CH_3	CH_2	N	O	377	311	299	283	113	114	99	84	72
T-SDF	H	CH_2	N	S	393	327	315	299	99	100	-	70	58
HH-SDF	CH_2OH	CH_2	N	O	377	311	299	283	129	130	99	100	88
NR-SDF	-	-	CH_2	O	377	311	299	283	84	85	-	-	-
H-SDF-d_3	CD_3	CD_2	N	O	377	311	299	283	118	119	101	89	77

Scheme 1. Fragmentation scheme for sildenafil and analogues.

processes and are discharged as parent compound, and possibly metabolites, eventually into sewage. Recent monitoring studies conducted on raw and treated sewage from municipal wastewater treatment plants (WWTP) have provided evidence for the occurrence of PDE-5 inhibitors, including SDF and several human metabolites.[13,14] As with many other human pharmaceuticals, common sewage treatment does not completely remove these compounds from the wastewater stream and eventually leads to discharge into receiving water bodies.[15] Once the aquatic environment has been reached, their fate is governed by a combination of biotic and abiotic processes. Into the latter category fall photochemical reactions which are considered an important mechanism in the natural attenuation of organic environmental micropollutants.[16] To address the possibility of photolysis of PDE-5 inhibitors in the environment, recent research efforts in our group were devoted to assessing the photodegradability of SDF under simulated sunlight.[17] In these studies we could demonstrate that the aliphatic piperazine ring was the principal target of the photolytical processes. With the aid of high-resolution mass spectrometry (quadrupole-time of flight instrument), coupled to ultra-high performance liquid chromatography (UHPLC), a total of 18 photoproducts could be identified through their unique mass spectral fragmentation patterns.

With this in mind, the current work builds on the outcomes of the previous study and aims to extend the spectrum of investigated compounds by including a number of structural derivatives of SDF, all of which reported to occur as analogs of erectile dysfunction drugs in various natural herbal products.[1,18–21] Specifically, the objective consisted of elucidating the phototransformation reactions of the four SDF analogs H-SDF, HH-SDF, T-SDF and NR-SDF (Scheme 1), in aqueous solution under the influence of simulated solar radiation. Based on the findings of the SDF studies,[17] we expected that the photodegradation pathways for the former three compounds (NR-SDF does not contain a piperazine ring in its structure), and therefore the spectra of their intermediates formed were very similar to those identified for SDF with a first generation quadrupole time-of-flight MS instrument. Largely improved sensitivity, resolution and mass accuracy of the Q Exactive-Orbitrap-MS platform held great promise in achieving more robust identification results.

Experimental

Chemical reagents

SDF, DM-SDF, H-SDF, H-SDF-d_5, HH-SDF, NR-SDF and T-SDF were purchased from Toronto Research Chemicals (Toronto, Canada). All organic solvents used for UPLC and TLC were Chromasol LC grade or equivalent. Ultra pure water and LC/MS grade formic acid were purchased from Sigma Aldrich (Munich, Germany). LC-grade acetonitrile was purchased from Riedel de Häen (Steinheim, Germany).

Photolysis experiments

Phototransformation experiments were conducted in a Suntest CPS solar simulator (Heraeus, Hanau, Germany) equipped with a Xenon lamp. Appropriate window glass filters were installed between the light source and the test solution in order to generate an emission spectrum similar to that of natural solar radiation. Test solutions of H-SDF, HH-SDF, NR-SDF and T-SDF at 10 mg/l and 1 μg/l were prepared in artificial freshwater (AFW) resembling a moderately hard water (96 mg/l $NaHCO_3$, 60 mg/l $CaSO_4{\cdot}2H_2O$, 60 mg/l $MgSO_4$ and 4 mg/l KCl; pH: 6.9). Test solutions were irradiated in capped quartz tubes (not airtight) for up to 58 h. Dark control solutions containing the target analytes and the selected matrix were kept inside the exposure chamber to mimic the temperature conditions. Subsamples of dark controls were taken at the same time points as those from the irradiation experiments. H-SDF, HH-SDF, NR-SDF and T-SDF concentrations remained constant in the dark controls over the test period and no bio or thermal degradation products were observed in the vials (data not shown).

Sampling and sample preparation

Reclaimed water (16 l) from the North District Wastewater Treatment Plant (North Miami, FL) was collected during the month of June of 2014 in pre-cleaned stainless steel containers. The sample produced reclaimed water for irrigation by using primary and secondary treatment followed by final disinfection. Because the nature and functionalities of the metabolites targeted was completely unknown sample extraction was performed in three 4-l aliquots by liquid–liquid extraction against methylene chloride.

Journal of MASS SPECTROMETRY

For two of the aliquots pH was modified prior to extraction as follows: aliquot A was acidified to pH 3.56 using 200 µl of formic acid; aliquot B was basified to pH 9.66 using 3000 µl of ammonium hydroxide. Aliquot C was extracted as untreated (neutral). Liquid–liquid extractions were performed using multiple 2-l separatory funnels, and analytes were extracted using a total of 300 mL of methylene chloride (3 x 100 mL) per sample aliquot. Extracts were dried over anhydrous sodium sulfate and their volumes reduced to 1000 µl of methylene chloride using a combination of a water bath and a stream of purified nitrogen gas. Prior to analysis the extracts with UPLC-HR-MS (see next section) were diluted with a mixture of methanol and water containing a suitable modifier such as formic acid of ammonium formate.

UHPLC/ESI-MS/MS analysis

Photolysis samples

Chromatographic separation was performed on a Waters ACQUITY BEH C_{18} column (50 × 2.1 mm, 1.7-µm particle size) equipped with a guard column (5 × 2.1 mm) of the same packing material. The mobile phases were (A) 0.1% HCOOH or 20 mM of NH_4OAc for acid and neutral conditions respectively, and (B) acetonitrile. After 0.5-min isocratic elution at 90% A, the proportion of A was linearly decreased to 10% within 6.5 min. The percentage of A was then maintained at 10% and held for 1.0 min. The initial mobile phase composition was reestablished within 1.0 min followed by a 2.0-min equilibration step at 90% A. The flow rate was 300 µl/min, and the injection volume was 10 µl. Exact mass measurements of the SDF analogs and their phototransformation products formed in the irradiation device were carried out in full-scan and product ion scan mode on a Q Exactive mass spectrometer (Thermo Fisher Scientific, San Jose, CA, USA). All MS experiments were performed in the positive ion mode using Heated Electro Spray Ionization (HESI). The source parameters were as follows: spray voltage: +3000 V; sheath gas pressure: 40 psi; auxiliary gas flow: 10 (arbitrary units); capillary temperature: 350 °C; heater temperature: 300 °C. The Orbitrap mass analyzer was operated at a resolving power of 70 000 (FWHM) in full-scan mode and of 17 500 (FWHM) in the data-dependent MS^2 mode (normalized collision energy of 40). The accurate mass of diisooctyl phthalate (*m/z* 391.28429) as a ubiquitous contaminant in LC-MS systems was used as a lock mass. External mass calibration for positive ESI mode was conducted every 5 days for the mass range of *m/z* 50–2000 by infusing a Pierce LTQ Velos ESI Positive Ion calibration solution from Thermo Fisher Scientific. All MS data acquisition and processing were done using the software package Xcalibur 2.2.

Environmental samples

Liquid chromatography analysis was carried out using a quaternary Accela 1200 pump equipped with a CTC PAL autosampler. Twenty microliters of the extract was used for analysis. Separation of analytes was achieved using a Hypersil Gold aQ (150 × 2.1 mm × 3 µm) analytical column and a gradient composition of methanol, HPLC grade water and HPLC water with 1% formic acid and 100 mM ammonium formate. Detection of analytes was performed using a Thermo QExactive Orbitrap high resolution mass spectrometer equipped with a HESI ionization source operated in the positive mode. Full scan analysis (R = 140 000) followed by target MS2 analysis (R = 35 000, NCE 35) was carried out for identification and confirmation purposes. Samples were acquired in both ESI positive and negative ion mode and processed for target compound identification using a combination of Xcalibur, Metworks and Mass Frontier software packages (Thermo Scientific, San Jose CA).

Results and discussion

Irradiation of the aqueous solutions degraded efficiently undeclared erectile dysfunction drugs in all studied matrices at high and low concentration. Figure S1, provided in the Supporting Information, shows the degradation profiles at different concentrations. Common phototransformation products were obtained in each sample, regardless of the concentration of the test compound (Figure S4). Plausible chemical structures were proposed by combining chromatographic information, accurate mass and MS^2 fragmentation data based on the knowledge of the photodegradation pathways of SDF.[17]

Comparison of the TICs of the control samples with those of the irradiated samples showed several new peaks indicating the presence of phototransformation products (Fig. S2). Their retention times relative to the test compound provided first hints on the polarity of the photodegradates. *N*-Oxide-SDF was confirmed with a chemically synthetized standard in the irradiated samples from T-SDF. In order to identify the formation of more *N*-oxides of the two other piperazine-analogs of SDF (H-SDF and HH-SDF), the change of pH of the mobile phase was evaluated. Figure S3 compares the effect of mobile phase pH (3.2 *vs* 6.8) on the retention times of H-SDF and TP504. In case of H-SDF increasing the pH from 3.2 to 6.8 led in stronger retention. This behavior was expected because the lower degree of protonation of the tertiary amine (pK_b) in the piperazine ring resulted in a less polar molecule. Results indicated that the new TP corresponds to a neutral molecule probably to an *N*-oxide. If other polar compounds would have been formed, when changing the pH of the mobile phase a shift in the retention time of the new TP on the reversed-phase column would have been observed. The effect of the pH on the retention times of TPs allow us to gain insight on the formation of *N*-oxides of the two analogs containing the piperazine ring in their structures.[22,23]

Fragmentation patterns of H-SDF, HH-SDF, T-SDF and NR-SDF

In order to identify the structures of the TPs formed under simulated sunlight, the first step was to elucidate and compare the fragmentation patterns of the four related parent compounds obtained under (+)ESI conditions. The high-resolving Q Exactive mass spectrometer delivered consistently low mass errors in both full-scan and product ion mode, thereby greatly facilitating the assignment of fragment ion compositions (Tables 1 and 2). Moreover, previous experience gained on a QToF-MS for SDF and its photoproducts allowed for straightforward interpretation of the (+)ESI-MS^2 spectra (for the sake of comparability Fig. 1 includes the mass spectrum of SDF).[17,24] The generic fragmentation pathway depicted in Scheme 1 summarizes the main fragment ions. While the right portion of the molecule containing the phenyl-pyrazolopyrimidin (ethi)one remains largely intact upon collision-induced dissociation, several bond cleavages occur at, and in the proximity of, the sulfonamide bond as well as within the piperazine ring. The fragmentations ***a***, ***b***, ***c*** and ***d*** lead to a characteristic set of ions with *m/z* ratios of 377, 311, 299 and 283 for SDF, H-SDF, HH-SDF and NR-SDF. In T-SDF where the oxygen atom of the pyrimidinone ring is replaced by a sulfur atom, the corresponding cleavages produce fragment ions that are 16 *m/z* units heavier (*m/z* 393 (***a***), 327 (***b***), 315 (***c***) and 299 (***d***)). Given the distinct substitution pattern in the piperazine

Table 1. Accurate mass measurements of H-SDF($-d_5$), HH-SDF, T-SDF and NR-SDF obtained by UPLC-(+)ESI-Orbitrap-MS in MS or MS/MS mode

Compound	Measured ion mass [*m/z*]	Elemental composition	Theoretical ion mass [*m/z*]	Rel. error [ppm]
H-SDF	489.2281	$C_{23}H_{33}N_6O_4S$	489.2279	0.5
	461.1969	$C_{21}H_{29}N_6O_4S$	461.1966	0.8
	377.1281	$C_{17}H_{21}N_4O_4S$	377.1278	0.7
	311.1503	$C_{17}H_{19}N_4O_2$	311.1503	0.2
	283.1195	$C_{15}H_{15}N_4O_2$	283.1190	1.8
	113.1078	$C_6H_{13}N_2$	113.1073	3.8
	99.0923	$C_5H_{11}N_2$	99.0917	5.8
	84.0815	$C_5H_{10}N$	84.0808	8.1
	72.0816	$C_4H_{10}N$	72.0808	10.7
	58.0660	C_3H_8N	58.0651	15.4
H-SDF-d_5	494.2589	$C_{23}H_{28}D_5N_6O_4S$	494.2592	0.6
	461.1973	$C_{21}H_{29}N_6O_4S$	461.1966	1.7
	377.1284	$C_{17}H_{21}N_4O_4S$	377.1278	1.6
	311.1500	$C_{17}H_{19}N_4O_2$	311.1503	−0.9
	283.1188	$C_{15}H_{15}N_4O_2$	283.1190	−0.4
	118.1391	$C_6H_8D_5N_2$	118.1387	3.0
	101.1047	$C_5H_9D_2N_2$	101.1042	4.7
	89.1128	$C_5H_5D_5N$	89.1122	7.5
	77.1129	$C_4H_5D_5N$	77.1122	10.0
	62.0911	$C_3H_4D_4N$	62.0902	14.0
HH-SDF	505.2232	$C_{23}H_{33}N_6O_5S$	505.2228	0.9
	487.2129	$C_{23}H_{31}N_6O_4S$	487.2122	1.5
	461.1970	$C_{21}H_{29}N_6O_4S$	461.1966	1.0
	377.1281	$C_{17}H_{21}N_4O_4S$	377.1278	0.8
	311.1505	$C_{17}H_{19}N_4O_2$	311.1503	0.6
	299.1142	$C_{15}H_{15}N_4O_3$	299.1139	1.2
	283.1192	$C_{15}H_{15}N_4O_2$	283.1190	0.9
	129.1026	$C_6H_{13}N_2O$	129.1022	2.9
	112.1000	$C_6H_{10}NO$	112.0757	4.5
	99.0923	$C_5H_{11}N_2$	99.0917	6.3
	88.0765	$C_4H_{10}NO$	88.0757	9.0
	74.0609	C_3H_8NO	74.0600	11.6
	58.0661	C_3H_8N	58.0651	16.3
T-SDF	491.1896	$C_{22}H_{31}N_6O_3S_2$	491.1894	0.6
	393.1046	$C_{17}H_{21}N_4O_3S_2$	393.1050	−0.8
	327.1274	$C_{17}H_{19}N_4OS$	327.1274	−0.1
	299.1138	$C_{15}H_{15}N_4OS$	299.1139	0.4
	100.1002	$C_5H_{12}N_2$	100.0995	6.5
	99.0923	$C_5H_{11}N_2$	99.0917	6.4
	85.0767	$C_4H_9N_2$	85.0760	8.4
	70.0660	C_4H_8N	70.1651	11.8
	58.0660	C_3H_8N	58.0651	15.2
NR-SDF	460.2015	$C_{22}H_{30}N_5O_4S$	460.2013	0.4
	432.1702	$C_{20}H_{26}N_5O_4S$	432.1700	0.5
	377.1274	$C_{17}H_{21}N_4O_4S$	377.1278	−1.0
	329.1611	$C_{17}H_{21}N_4O_3$	329.1608	1.0
	311.1504	$C_{17}H_{19}N_4O_2$	311.1503	0.6
	299.1142	$C_{15}H_{15}N_4O_3$	299.1139	1.0
	283.1193	$C_{15}H_{15}N_4O_2$	283.1190	1.2
	256.0953	$C_{13}H_{12}N_4O_2$	256.0955	−0.8
	84.0815	$C_5H_{10}N$	84.0808	8.6

ring (piperidine in case of NR-SDF) of the SDF analogs, fragment ions arising from cleavage of the sulfonamide bond (***e***) or dissociation of the aliphatic ring (***f***, ***g*** and ***h***) have compound-specific *m/z* values. All

Table 2. Accurate mass measurements of photoproducts obtained by UPLC-(+)ESI-Orbitrap-MS in MS or MS/MS mode. For those TPs formed by more than one parent compound the listed data correspond to the one labeled with an asterisk. The accurate mass data for the other parent compounds are provided in Tables S1, 2 and 3 in the Supporting Information

Photoproduct	Formed by…	Measured ion mass [*m/z*]	Elemental composition	Theoretical ion mass [*m/z*]	Rel. error [ppm]
TP520	HH-SDF	521.2182	$C_{23}H_{33}N_6O_6S$	521.2177	1.0
		473.1975	$C_{22}H_{29}N_6O_4S$	473.1966	2.0
		404.1389	$C_{18}H_{22}N_5O_4S$	404.1387	0.4
		377.1282	$C_{17}H_{21}N_4O_4S$	377.1278	1.1
		344.1482	$C_{17}H_{20}N_4O_4$	344.1479	1.0
		311.1502	$C_{17}H_{19}N_4O_2$	311.1503	0.1
		283.1191	$C_{15}H_{15}N_4O_2$	283.1190	0.6
		129.1025	$C_6H_{13}N_2O$	129.1022	2.3
		98.0846	$C_5H_{10}N_2$	98.0839	7.2
		83.0611	$C_4H_7N_2$	83.0604	9.3
TP506	HH-SDF	507.2026	$C_{22}H_{31}N_6O_6S$	507.2020	1.0
		489.1926	$C_{22}H_{29}N_6O_5S$	489.1915	2.3
		461.1969	$C_{21}H_{29}N_6O_4S$	461.1966	0.6
		418.1552	$C_{19}H_{24}N_5O_4S$	418.1544	2.0
		311.1507	$C_{17}H_{19}N_4O_2$	311.1503	1.4
		299.1143	$C_{15}H_{15}N_4O_3$	299.1139	1.5
		283.1196	$C_{15}H_{15}N_4O_2$	283.1190	2.4
		115.0871	$C_5H_{11}N_2O$	115.0860	4.3
		88.0765	$C_4H_{10}NO$	88.0757	9.5
		70.0661	C_4H_8N	70.0651	13.6
TP504	H-SDF	505.2230	$C_{23}H_{33}N_6O_5S$	505.2228	0.2
		477.1918	$C_{21}H_{29}N_6O_5S$	477.1915	0.8
		404.1388	$C_{18}H_{22}N_5O_4S$	404.1387	0.1
		377.1278	$C_{17}H_{21}N_4O_4S$	377.1278	0.1
		344.1479	$C_{17}H_{20}N_4O_4$	344.1479	−0.1
		311.1501	$C_{17}H_{19}N_4O_2$	311.1503	−0.4
		283.1190	$C_{15}H_{15}N_4O_2$	283.1190	0.1
		113.1078	$C_6H_{13}N_2$	113.1073	3.8
		98.0845	$C_5H_{10}N_2$	98.0839	6.2
		83.0611	$C_4H_7N_2$	83.0604	8.3
TP490-A	H-SDF	491.2075	$C_{22}H_{31}N_6O_5S$	491.2071	0.7
		473.1972	$C_{22}H_{29}N_6O_4S$	473.1966	1.4
		463.2127	$C_{21}H_{31}N_6O_4S$	463.2122	1.1
		99.0924	$C_5H_{11}N_2$	99.0917	6.8
		72.0816	$C_4H_{10}N$	72.0808	11.8
TP490-B	T-SDF	491.2073	$C_{22}H_{31}N_6O_5S$	491.2071	0.4
		463.1756	$C_{20}H_{27}N_6O_5S$	463.1758	−0.4
		404.1389	$C_{18}H_{22}N_5O_4S$	404.1387	0.5
		377.1279	$C_{17}H_{21}N_4O_4S$	377.1278	0.3
		344.1479	$C_{17}H_{20}N_4O_4$	344.1479	−0.1
		311.1501	$C_{17}H_{19}N_4O_2$	311.1503	−0.5
		299.1138	$C_{15}H_{15}N_4O_3$	299.1139	−0.3
		283.1190	$C_{15}H_{15}N_4O_2$	283.1190	0.3
		99.0922	$C_5H_{11}N_2$	99.0917	5.1
		70.0659	C_4H_8N	70.1651	11.5
		58.0660	C_3H_8N	58.0651	14.9
TP488	H-SDF[a]	489.1919	$C_{22}H_{29}N_6O_5S$	489.1915	0.8
	HH-SDF	461.1970	$C_{21}H_{29}N_6O_4S$	461.1966	0.9
	T-SDF	377.1279	$C_{17}H_{21}N_4O_4S$	377.1278	0.2
		311.1507	$C_{17}H_{19}N_4O_2$	311.1503	1.3
		299.1146	$C_{15}H_{15}N_4O_3$	299.1139	2.3

(Continues)

Journal of MASS SPECTROMETRY

Table 2. (Continued)

Photoproduct	Formed by…	Measured ion mass [*m/z*]	Elemental composition	Theoretical ion mass [*m/z*]	Rel. error [ppm]
		283.1195	$C_{15}H_{15}N_4O_2$	283.1190	1.9
		85.0768	$C_4H_9N_2$	85.0760	9.6
TP478	HH-SDF	479.2074	$C_{21}H_{31}N_6O_5S$	479.2071	0.6
		461.1964	$C_{21}H_{29}N_6O_4S$	461.1966	−0.3
		418.1550	$C_{19}H_{24}N_5O_4S$	418.1544	1.6
		435.1813	$C_{19}H_{27}N_6O_4S$	435.1809	1.0
		392.1394	$C_{17}H_{22}N_5O_4S$	392.1387	1.7
		344.1488	$C_{17}H_{20}N_4O_4$	344.1479	2.6
		311.1502	$C_{17}H_{19}N_4O_2$	311.1503	−0.2
		299.1140	$C_{15}H_{15}N_4O_3$	299.1139	0.5
		283.1192	$C_{15}H_{15}N_4O_2$	283.1190	0.8
		149.0383	$C_4H_9N_2O_2S$	149.0379	2.5
		88.0764	$C_4H_{10}NO$	88.0757	7.5
		70.06595	C_4H_8N	70.0651	11.8
TP476	T-SDF	477.1917	$C_{21}H_{29}N_6O_5S$	477.1915	0.5
		449.1971	$C_{20}H_{29}N_6O_4S$	449.1966	1.2
		418.1545	$C_{19}H_{24}N_5O_4S$	418.1544	0.3
		392.1393	$C_{17}H_{22}N_5O_4S$	392.1387	1.4
		311.1504	$C_{17}H_{19}N_4O_2$	311.1503	0.4
		283.1193	$C_{15}H_{15}N_4O_2$	283.1190	1.4
		85.0768	$C_4H_9N_2$	85.0760	9.6
		58.0661	C_3H_8N	58.0651	16.1
TP474 (SDF)	T-SDF	475.2125	$C_{22}H_{31}N_6O_4S$	475.2122	0.6
		377.1287	$C_{17}H_{21}N_4O_4S$	377.1278	2.4
		311.1505	$C_{17}H_{19}N_4O_2$	311.1503	0.8
		283.1193	$C_{15}H_{15}N_4O_2$	283.1190	1.4
		100.1001	$C_5H_{12}N_2$	100.0995	6.3
		99.0923	$C_5H_{11}N_2$	99.0917	6.2
		70.0660	C_4H_8N	70.1651	11.8
		58.0660	C_3H_8N	58.0651	15.7
TP462-A	H-SDF	463.2124	$C_{21}H_{31}N_6O_4S$	463.2122	0.3
		435.1829	$C_{19}H_{27}N_6O_4S$	435.1809	4.6
		418.1548	$C_{19}H_{24}N_5O_4S$	418.1544	1.0
		392.1382	$C_{17}H_{22}N_5O_4S$	392.1387	−1.3
		344.1486	$C_{17}H_{20}N_4O_4$	344.1479	2.0
		311.1502	$C_{17}H_{19}N_4O_2$	311.1503	−0.1
		299.1142	$C_{15}H_{15}N_4O_3$	299.1139	1.0
		283.1193	$C_{15}H_{15}N_4O_2$	283.1190	1.2
		151.0537	$C_4H_{11}N_2O_2S$	151.0536	0.9
		72.0816	$C_4H_{10}N$	72.0808	11.4
		58.0660	C_3H_8N	58.0651	15.7
TP462-B	H-SDF[a]	463.1760	$C_{20}H_{27}N_6O_5S$	463.1758	0.4
	HH-SDF	435.1811	$C_{19}H_{27}N_6O_4S$	435.1809	0.4
	T-SDF	418.1545	$C_{19}H_{24}N_5O_4S$	418.1544	0.4
		393.1223	$C_{17}H_{21}N_4O_5S$	393.1227	−1.1
		311.1502	$C_{17}H_{19}N_4O_2$	311.1503	−0.1
		299.1142	$C_{15}H_{15}N_4O_3$	299.1139	1.0
		283.1193	$C_{15}H_{15}N_4O_2$	283.1190	1.1
		71.0611	$C_3H_7N_2$	71.0604	10.2
		59.0612	$C_2H_7N_2$	59.0604	13.5
TP460	H-SDF[a]	461.1967	$C_{21}H_{29}N_6O_4S$	461.1966	0.2
	HH-SDF	377.1278	$C_{17}H_{21}N_4O_4S$	377.1278	0.1
	T-SDF	311.1507	$C_{17}H_{19}N_4O_2$	311.1503	1.4
		299.1140	$C_{15}H_{15}N_4O_3$	299.1139	0.6

(Continues)

Table 2. (Continued)

Photoproduct	Formed by…	Measured ion mass [*m/z*]	Elemental composition	Theoretical ion mass [*m/z*]	Rel. error [ppm]
		283.1195	$C_{15}H_{15}N_4O_2$	283.1190	1.8
		85.0768	$C_4H_9N_2$	85.0760	9.3
TP448	T-SDF	449.1968	$C_{20}H_{29}N_6O_4S$	449.1966	0.4
		418.1546	$C_{19}H_{24}N_5O_4S$	418.1544	0.6
		392.1389	$C_{17}H_{22}N_5O_4S$	392.1387	0.4
		377.1278	$C_{17}H_{21}N_4O_4S$	377.1278	−0.1
		311.1502	$C_{17}H_{19}N_4O_2$	311.1503	−0.3
		283.1189	$C_{15}H_{15}N_4O_2$	283.1190	−0.1
		137.0375	$C_3H_9N_2O_2S$	137.0379	−2.8
		73.0768	$C_3H_9N_2$	73.0760	10.5
		58.0660	C_3H_8N	58.0651	14.4
TP434	H-SDF[a]	435.1811	$C_{19}H_{27}N_6O_4S$	435.1809	0.4
	HH-SDF	418.1545	$C_{19}H_{24}N_5O_4S$	418.1544	0.5
	T-SDF	392.1386	$C_{17}H_{22}N_5O_4S$	392.1387	−0.4
		377.1285	$C_{17}H_{21}N_4O_4S$	377.1278	1.7
		311.1502	$C_{17}H_{19}N_4O_2$	311.1503	−0.1
		299.1141	$C_{15}H_{15}N_4O_3$	299.1139	0.8
		283.1191	$C_{15}H_{15}N_4O_2$	283.1190	0.5
TP392	H-SDF[a]	393.1224	$C_{17}H_{21}N_4O_5S$	393.1227	−0.8
	HH-SDF	365.0916	$C_{15}H_{17}N_4O_5S$	365.0914	0.5
	T-SDF	336.0521	$C_{13}H_{12}N_4O_5S$	336.0523	−0.7
	NR-SDF	284.1269	$C_{15}H_{16}N_4O_2$	284.1268	0.4
		256.0956	$C_{13}H_{12}N_4O_2$	256.0955	0.4
TP391	H-SDF[a]	392.1386	$C_{17}H_{22}N_5O_4S$	392.1387	−0.3
	HH-SDF	364.1078	$C_{15}H_{18}N_5O_4S$	364.1074	1.2
		335.0683	$C_{13}H_{13}N_5O_4S$	335.0683	0.1
		311.1505	$C_{17}H_{19}N_4O_2$	311.1503	0.7
	T-SDF	299.1140	$C_{15}H_{15}N_4O_3$	299.1139	0.4
	NR-SDF	283.1192	$C_{15}H_{15}N_4O_2$	283.1190	1.0
		256.0955	$C_{13}H_{12}N_4O_2$	256.0955	0.1

[a]Homolytic cleavage of sulfonamide bond.

of the analytes undergo cleavage of the sulfonamide bond according to ***e*** – in contrast to pathway ***a*** the positive charge remains in the left part of the molecule – but the cross-ring cleavages ***g*** and ***h*** are exclusively observed for the piperazine-bearing compounds (SDF, H-SDF, HH-SDF and T-SDF; $X_3 = N$ in generic structure in Scheme 1) in which. That NR-SDF does not produce any charged species apart from *m/z* 84 (see Fig. 1E) is due to the lack of a readily protonatable nitrogen in this moiety. It is worth mentioning that the dissociation of the sulfonamide bond according to the aforementioned pathway ***e*** can also proceed homolytically (indicated as ***e**** in Scheme 1), thereby generating radical cations that differ from the ions in series ***e*** by an additional hydrogen atom.

As there are a few subtle yet distinct features present in the mass spectra of the SDF analogs, closer examination of commonalities and differences is warranted. The mass spectra of both SDF and its thio-analog T-SDF show expectedly the formation of the ions at *m/z* 99 (100) and *m/z* 58 originating from fragmentations $\boldsymbol{e}^{(*)}$ and ***h***, respectively. Replacement of the *N*-methyl group by an ethyl group in H-SDF (Fig. 1A), in turn, leads to the homologues ions at *m/z* 113 (114) and *m/z* 72 in the (+)ESI-MS^2 spectrum. Unexpected though is the observation of intense ions with *m/z 99* and *m/z* 58 which differ from the two former ions by a CH_2 unit. What at first glance suggests cross-ring cleavage involving rupture of the C—C

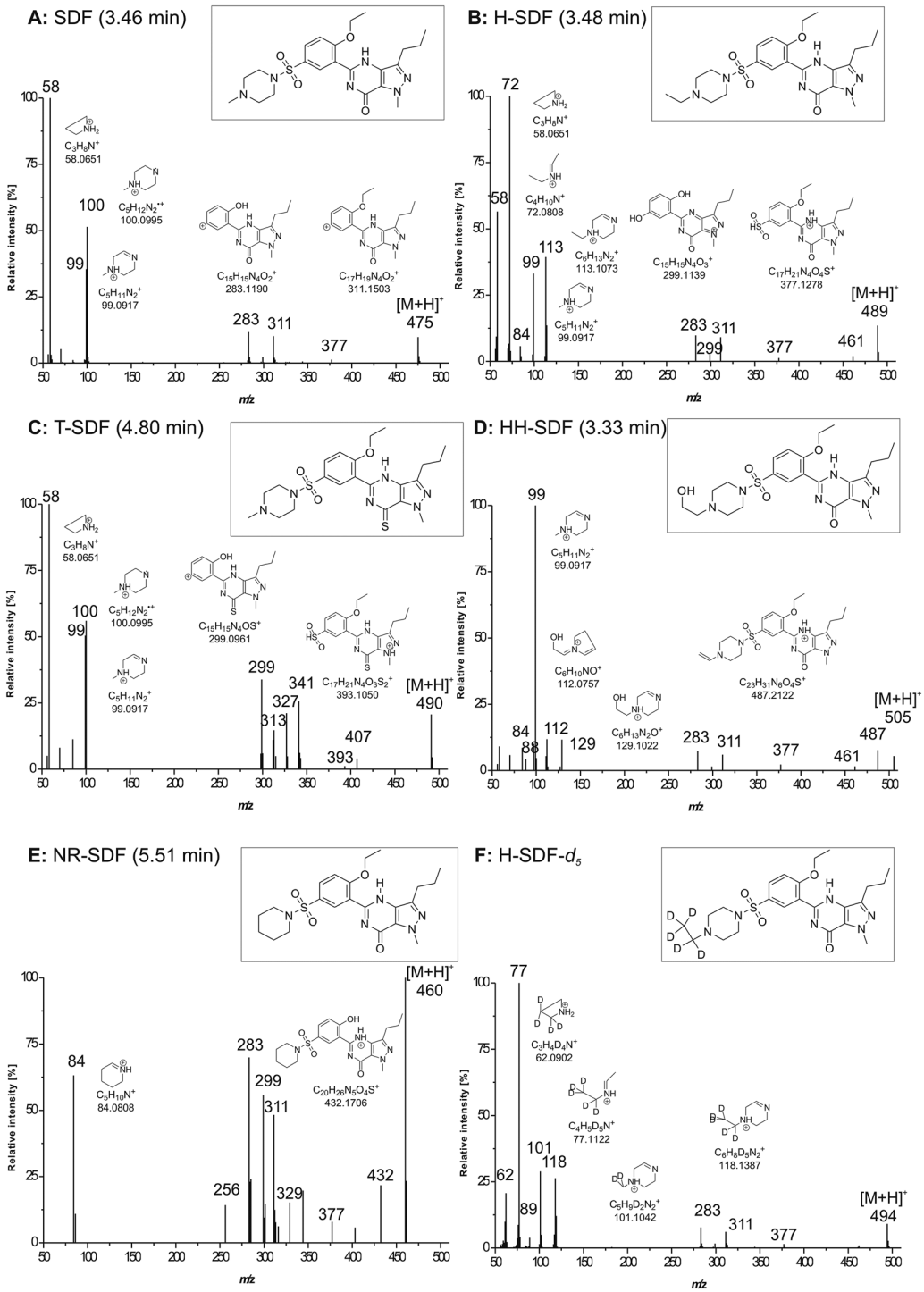

Figure 1. (+)ESI-MS/MS spectra of SDF, H-SDF, T-SDF, HH-SDF, NR-SDF and H-SDF-d_5.

bond in the ethylene bridge of the piperazine ring corresponds in fact to elimination of the terminal methyl group. By recording the (+)ESI product ion mass spectrum of H-SDF-d_5, the mass shifts relative to H-SDF provide valuable information on the site of fragmentation. In H-SDF-d_5 all five deuterium atoms are located in the *N*-ethyl group. Therefore, the fragmentations ***a***, ***b***, ***c*** and ***d*** produce the same set of ions as in H-SDF (see Scheme 1). On the other hand, the ions *m/z* 118 and 77 in the spectrum of H-SDF-d_5 are 5 *m/z* units higher than the corresponding ions in the H-SDF product ion profile, being in line with conservation of all five deuterium atoms in these two ion species. Determination of the elemental composition of the ion at *m/z* 101, however, reveals the presence of only two deuterium atoms in this ion ($C_5H_9D_2N_2$) thus providing evidence for loss of the CD_3 group at some point during the collision-induced dissociation. As for the fragment ion *m/z* 62, the accurate mass data suggest a formula of $C_3H_4D_4N$, i.e. one deuterium has been lost during the fragmentation process. The inset in Fig. 1C shows a plausible structure of this ion in which rearrangement has led to a four-membered ring. As far as *N*-hydroxyethyl analog HH-SDF is concerned (Fig. 1D), the

Journal of MASS SPECTROMETRY

protonated molecule can undergo dehydration of the aliphatic hydroxyl group to generate *m/z* 487. Cleavage of the precursor ion according to pathway ***e*** gives rise to ion *m/z* 129. The base peak in the mass spectrum (*m/z* 99) corresponds to the formula $C_5H_{11}N_2$ thus being identical in composition to *m/z* 99 in SDF. It is proposed to correspond to the elimination of methanol (30 Da) from *m/z* 129. A fragment ion with a unique structure is detected at *m/z* 112. Here, the accurate mass strongly points at simultaneous cleavage of the C—N bonds between the carbons of the two ethylene groups and the sulfonamide-N. To produce an unsubstituted sulfonamide as neutral fragment, two hydrogen atoms have to be transferred to the sulfonamide-N, thereby generating the unsaturated species shown in the inset in Fig. 1C.

Identification of the photoproducts

Upon irradiation of the spiked AFW solutions with simulated sunlight, all four test compounds (H-SDF, HH-SDF, T-SDF and NR-SFD) underwent extensive photodegradation. The UPLC-based separation revealed the conversion of the SDF analogs into mixtures of different complexity. Compilation of retention time and molecular weight information provided already hints on the presence of several identical photoproducts across compounds. This came as no surprise because previous studies performed on SDF had demonstrated the gradual breakdown of the piperazine ring up to the point where hydrolysis of the sulfonamide yielded a stable sulfonic acid derivative. Since, with the exception of T-SDF, all other analogs bore modifications in this aliphatic heterocycle, its light-induced destruction would eventually lead to the generation of photoproducts with identical structures. In case of T-SDF none of the mass spectra of the photoproducts showed the diagnostic series of ions at *m/z* 299, 315, 327 and 393 produced by fragmentation of the protonated parent compound. Instead, they were all shifted to the SDF-specific series of *m/z* 283, 299, 313 and 377, and, in fact, SDF was unequivocally identified in the samples from the T-SDF photolysis experiments by the perfect match of retention time and product ion profile. The absence of thioketone-containing photoproducts indicated a rapid oxidation of this moiety and therefore allowed to anticipate a degradation pathway comparable to that of SDF.

The (+)ESI mass spectra of six photoproducts common to H-SDF, HH-SDF and T-SDF are depicted in Fig. 2 with the corresponding accurate mass data listed in the Table 2. The heaviest of them (TP488) had an elemental composition of $C_{22}H_{28}N_6O_5S$ and showed an intense fragment ion at *m/z* 461 corresponding to the loss of CO from the molecular íon (Fig. 2A). The same difference in *m/z* values and elemental compositions was observed between the low-intensity fragment ion at *m/z* 113 and the abundant ion with *m/z* 85. The accurate mass data of the latter indicated a composition of $C_4H_9N_2$ which led to propose the cyclic structure shown in the inset of Fig. 2-A. The dissociation of CO from the protonated molecule and from fragment ion *m/z* 113 is consistent with an amide that results from oxidation of the *N*-alkyl group in H-SDF, HH-SDF and T-SDF (converted into SDF after oxidation of the thioketone). Complete loss of the N-substituent is then postulated to generate TP460 exhibiting a very similar fragmentation pattern with the characteristic ion at *m/z* 85 (Fig. 2C). The formation of this secondary-amine bearing compound was ultimately confirmed by comparison with the authentic standard, N-demethylated SDF, which was commercially available and reported to be a major human metabolite of SDF. The TP434 ($C_{19}H_{26}N_6O_4S$) in turn differs in chemical formula from TP460 by the elimination of C2H2 and while it maintains the diagnostic series at *m/z* 283, 299, 311 and 377, it lacks prominent fragment ions in the low mass range (Fig. 2D). A key fragment ion in the mass spectrum of TP434 originates from loss of ammonia in the precursor ion which points at the presence of a terminal amine group as proposed in the *N,N*-deethylated structure shown in Fig. 2D. If dissociation of the sulfur-nitrogen bond in the sulfonamide group precedes the neutral loss of NH_3 from the precursor ion, the result is the low-intensity ion at *m/z* 59 (C_3H_8N). Further photo-induced degradation of TP434 upon loss of the aminoethyl substituent of the sulfonamide is then postulated to generate TP391 ($C_{17}H_{22}N_5O_4S$). With an unsubstituted sulfonamide remaining, no low-mass fragment íons are observed under the applied CID conditions (Fig. 2F). Instead, the first step of dissociation corresponds to the loss of ethylene producing the base peak at *m/z* 364 ($C_{15}H_{18}N_5O_4S$). This cleavage is proposed to occur in the ethoxy group in analogy to the difference in generic fragmentations ***b*** and ***d*** in Scheme 1 (see also inset in Fig. 1A). In contrast, fragmentation according to pathway ***a*** cannot take place in the N-unsubstituted sulfonamide TP391, and hence the class-specific fragment ion at *m/z* 377 is not anymore detected in the mass spectrum. The emergence of fragment ions at *m/z* 335 and 256, however, cannot be rationalized using straightforward heterolytic cleavages. Since the accurate mass data clearly point to chemical formulae of $C_{13}H_{13}N_5O_4S$ and $C_{13}H_{12}N_4O_2$, respectively (these two differ in composition by $HNSO_2$), the fact that computing the double-bond equivalents of these charged species produce integer values can only be attributed to the presence of ions with unpaired electrons. As for *m/z* 335, successive elimination from the molecular ion of first C_2H_4 (ethoxy group: *m/z* 364) and then of C_2H_5 from the propyl side chain give rise to this fragment ion bearing an exo-methylene group. The relative stability of this radical is thought to be due to resonance stabilization involving the adjacent imine group. The same sequence of neutral losses is apparent in the mass spectrum of TP392 (Fig. 2E) where a hydroxyl group replaces the amino group in the sulfonamide to yield the corresponding sulfonic acid ($C_{17}H_{20}N_4O_5S$). Under the applied CID conditions, the radical ion at *m/z* 256 – as in case of TP391 – represents the final stage of fragmentation.

Of the aforementioned photoproducts identified in the irradiated solutions of H-SDF, HH-SDF and T-SDF, only TP391 and TP392 were formed during exposure of NR-SDF in the sunlight simulator. This is fully in line with the structural differences between the four SDF analogs: lacking the tertiary amine, the *N,N*-pentylene bridge in NR-SDF does not give rise to any oxidative intermediates but produces directly the *N,N*-dealkylated compound TP391.

Beside those TPs that were observed for more than one of the test compounds, a number of unique photoproducts was detected suggesting the conservation of the substance-specific N-alkyl substituent on the respective piperazine rings. Comparison of the elemental compositions of the molecular ions as well as examination of the product ion spectra (Fig. 3) for commonalities revealed the presence of three series, of which the first one comprised TPs arising from monooxygenation (TP504 for H-SDF; TP520 for HH-SDF; TP490-B for T-SDF after conversion to SDF). With chromatographic retention times being longer than those of the test compounds (taking SDF as reference in case of T-SDF), C-hydroxylation on an aliphatic or aromatic position appeared unlikely as this would have generated more polar, and thus less retained, entities. At first glance the corresponding (+)ESI mass spectra (Fig. 3A, 3D and 3G) display an apparent inconsistency in that on the one hand they contain the characteristic series of ions comprising *m/z* 404, 311, 299 and 283

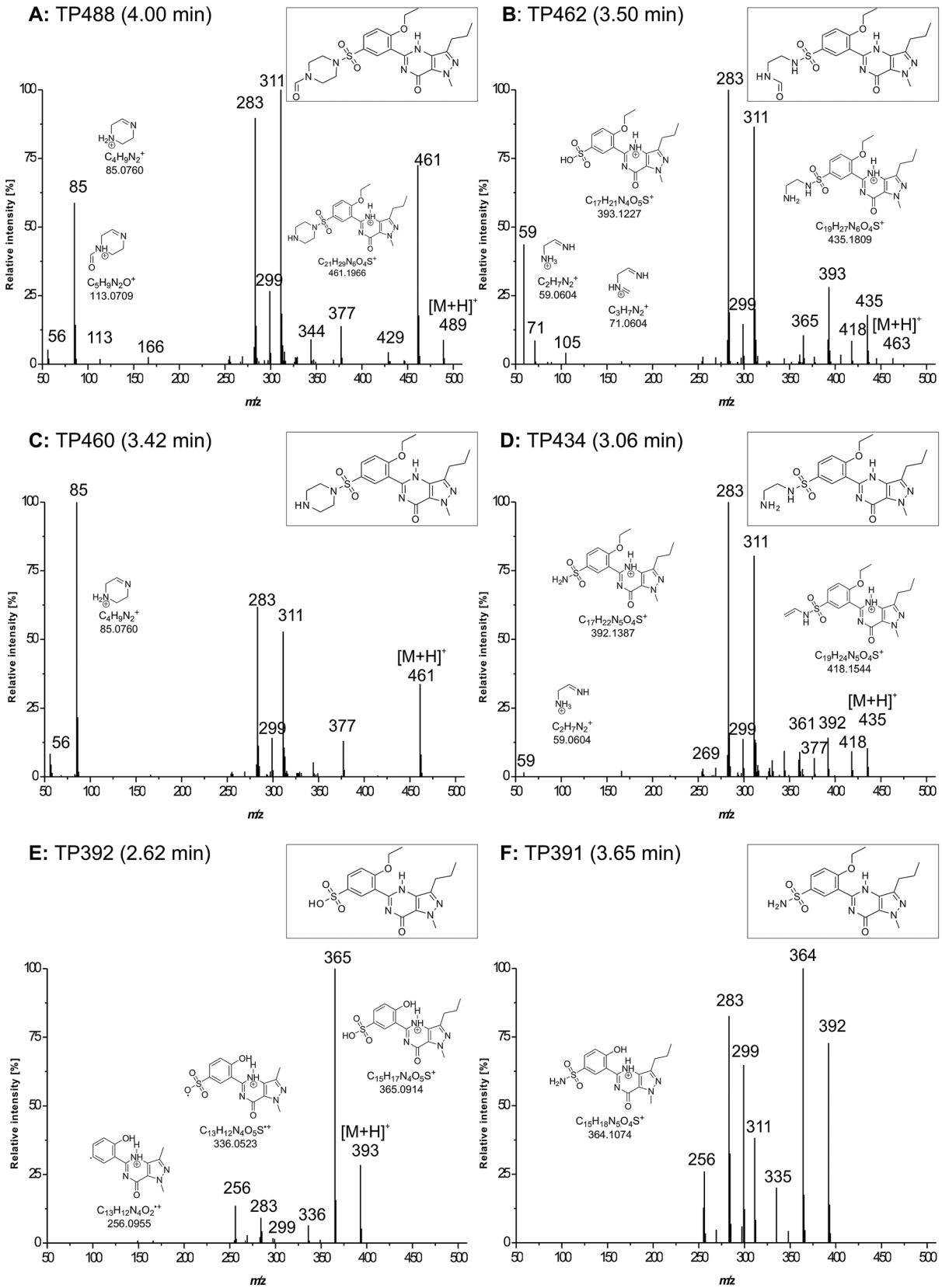

Figure 2. (+)ESI-MS/MS spectra of the common TPs obtained for H-SDF, HH-SDF and T-SDF irradiated samples.

indicating the absence of any modification beyond the sulfonamide, while on the other hand, fragment ions arising from cleavage according to process ***a*** in Scheme 1 are observed in all three spectra (*m/z* 113, 129 and 99, respectively). Based on compelling evidence presented in our previous work on the photodegradation of SDF under identical experimental conditions as in the current study,[17]

Journal of MASS SPECTROMETRY

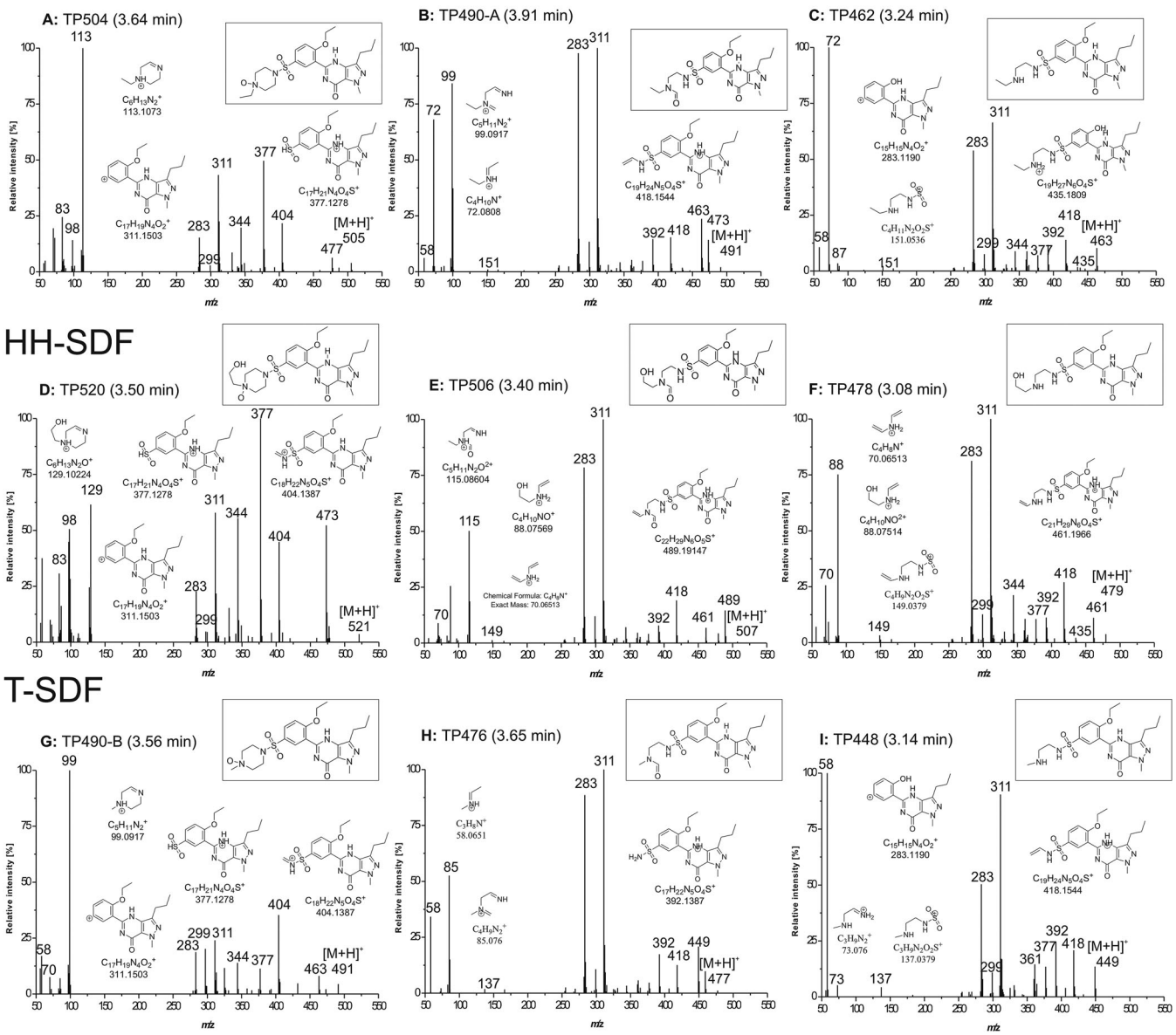

Figure 3. (+)ESI-MS/MS spectra of novel TPs obtained for H-SDF, HH-SDF and T-SDF irradiated samples.

the three TPs are attributed to N-oxygenation of the tertiary amine in the piperazine ring. In fact, the mass spectrum of TP490-B (Fig. 3G) is essentially identical to that of the eponymous photoproduct in Eichhorn *et al.*,[17] i.e. the N-oxide of SDF. As with TP490-B, formed from SDF after rapid initial oxidation of the thiocarbonyl group in T-SDF, the slower elution of TP504 and TP520 as compared to the precursor compound is due to the loss of basicity of the aliphatic amine by conversion into the neutral N-oxide.

Figure 3B, 3E and 3H shows a second series of TPs differing in elemental composition from the parent compounds (SDF in case of the T-SDF) by $-CH_2+O$. As with the three afore discussed TPs or in all three instances the fragment ions at *m/z* 283 and 311 indicate that the modification is in the left part of the molecule. As compared to the parent compounds, the piperazine ring-specific fragment ions at *m/z* 113, 129 and 99 (SDF) are shifted to *m/z* 99, 115 and 85 for H-SDF, HH-SDF and T-SDF (SDF), respectively. At the same time, the molecular ions of the TPs all show a loss of water producing *m/z* 473 (H-SDF), *m/z* 489 (HH-SDF) and *m/z* 459 (T-SDF/SDF) as well as decarbonilation of similar intensity. Plausible structures being consistent with these fragmentation patterns arise from oxidative cleavage of one ethylene bridge upon loss of one carbon atom. Fragmentation of the resulting amide produces the loss of CO or dehydration. Although the latter mechanism is uncommon, the loss of water from has been previously reported.[25]

A third series of homologous TPs comprises TP462 (H-SDF), TP478 (HH-SDF) and TP448 (T-SDF after oxidation to SDF). In terms of elemental formulae, they differ from their precursor compounds by removal of C_2H_2 (26 Da) (see Table 2). The heaviest fragment ion common to all three TPs (Fig. 3C, 3F, and 3I) is the even-electron species with *m/z* 418 ($C_{19}H_{24}N_5O_4S^+$). Taking into account that the three product ion spectra contain the characteristic series of ions at *m/z* 377, 311, 299 and 283, the most plausible photodegradation pathway giving rise to the TPs is *N,N*-deethylation. Hence, the

common ion at *m/z* 418 corresponds to the loss of the substituent on the secondary amine, e.g. of methylamine ($C_2H_5N = 31$ Da) in case of TP448. Apart from the mass spectral information, the chromatographic behavior is also in agreement with the structural modification insofar as the loss of lipophilicity, i.e. the bridging *N,N*-ethylene moiety, translates into weaker chromatographic retention and therefore earlier elution than the precursor compounds (H-SDF: 3.48 *vs* 3.64 min; HH-SDF: 3.33 *vs* 3.50 min; (T-)SDF: 3.46 *vs* 3.56 min).

Environmental occurrence

The environmental survey of SDF, SDF analogues and their TPs in waters allowed the first detection of TP488 and TP448 in effluent samples. SDF and SDF analogues were not detected in the effluent of WWTP and nor in surface waters. The implementation of UV treatment in the WWTPs could be an important factor in the formation of these TPs. Furthermore, these TPs could be produced from different treatments such as biodegradation in WWTP. Accurate masses and MS2 spectra are given in the Supporting Information (Figure S4) and confirmed TPs identities. Because authentic standards are currently not commercially available, the concentrations of TPs cannot be accurately determined.

Conclusion

In the present study, we examined the photodegradation pathways of several SDF analogues based on the elucidation of high-resolution MS/MS data. Thanks to distinct fragmentation patterns with a number of highly diagnostic fragment ions across the entire *m/z* range, and the possibility to rationalize the formation of the photoproducts by comparing the TP spectrum between the different SDF analogues, the structures of a large number of both unique and common photoproducts could be proposed. It was demonstrated that the piperazine-bearing analogues H-SDF, HH-SDF and T-SDF displayed a similar behavior as SDF in that the aliphatic ring was gradually broken down upon exposure to simulated sunlight. In case of the thioketone-containing T-SDF, all of the identified photoproducts were devoid of the C=S group thereby providing evidence for the instability of this moiety. With the thioketone being subject to rapid oxidation to the corresponding ketone group, i.e. becoming SDF, the set of generated photoproducts was therefore very similar to those reported in our previous work on the photolysis of SDF under identical experimental conditions. Lacking the basic nitrogen atom in the aliphatic ring, NR-SDF, in turn, gave rise to only two prominent photoproducts (TP391 and TP392). These were also found in the solutions of the experiments performed with H-SDF, HH-SDF and T-SDF indicating that the photodegradation pathways of all four SDF analogues eventually converged in the formation of the stable sulfonic acid TP392. Assuming that the findings from the photodegradation studies carried out under controlled laboratory conditions are predictive of the photofate under real conditions in the environment, e.g. in sunlit surface waters having received treated effluents from sewage treatment plants, the detection of one TP or another in the samples would likely not allow to unequivocally determine the identity of the discharged drug. On the other hand, the polar TP392 might serve as a tracer compound for detecting the contamination of surface waters with SDF-related compounds.

Environmental analysis allowed the first detection of TP488 and TP448 in wastewater effluents. It worth noting that their detection does not allow to unequivocally determine the identity of the initially discharged precursor compound, because the two TPs can originate from different SDF analogs.

Acknowledgements

This work has been supported by the Spanish Ministry of Science and Innovation [project Consolider-Ingenio 2010 Scarce CSD2009-00065]. This work reflects only the authors' views, and the European Community is not liable for any use that may be made of the information contained therein. SP acknowledges the contract from the Ramón y Cajal Program of the Spanish Ministry of Economy and Competitiveness. This work was partly financially supported by the Generalitat de Catalunya (Consolidated Research Group: Water and Soil Quality Unit 2014-SGR-418) and 2014 SGR 291-ICRA.

References

[1] B. J. Venhuis, D. de Kaste. Towards a decade of detecting new analogues of sildenafil, tadalafil and vardenafil in food supplements: A history, analytical aspects and health risks. *J. Pharm. Biomed. Anal.* **2012**, *69*, 196–208.
[2] S. Singh, B. Prasad, A. A. Savaliya, R. P. Shah, V. M. Gohil, A. Kaur. Strategies for characterizing sildenafil, vardenafil, tadalafil and their analogues in herbal dietary supplements, and detecting counterfeit products containing these drugs. *TrAC Trends Anal. Chem.* **2009**, *28*, 13–28.
[3] M. Y. Low, Y. Zeng, L. Li, X. W. Ge, R. Lee, B. C. Bloodworth, H. L. Koh. Safety and Quality Assessment of 175 Illegal Sexual Enhancement Products Seized in Red-Light Districts in Singapore. *Drug-Safety* **2009**, *32*, 1141–1146.
[4] M. H. Shin, M. K. Hong, W. S. Kim, Y. J. Lee, Y. C. Jeoung. Identification of a new analogue of sildenafil added illegally to a functional food marketed for penile erectile dysfunction. *Food Addit. Contam.* **2003**, *20*, 793–796.
[5] C. L. Kee, X. Ge, M.-Y. Low, H. L. Koh. Structural elucidation of a new sildenafil analogue using high-resolution Orbitrap mass spectrometry. *Rapid Commun. Mass Spectrom.* **2013**, *27*, 1380–1384.
[6] F. Shi, C. Guo, L. Gong, J. Li, P. Dong, J. Zhang, P. Cui, S. Jiang, Y. Zhao, S. Zeng. Application of a high resolution benchtop quadrupole-Orbitrap mass spectrometry for the rapid screening, confirmation and quantification of illegal adulterated phosphodiesterase-5 inhibitors in herbal medicines and dietary supplements, *J. Chromatogr. A. 1344*, 91–98.
[7] B. J. Venhuis, D. M. Barends, M. E. Zwaagstra, D.d. Kaste. Recent developments in counterfeits and imitations of Viagra, Cialis and Levitra, in: RIVM (Ed.), Bilthoven, 2000-2010.
[8] Y. C. Liao, K. C. Lai, H. C. Lee, Y. C. Liu, Y. L. Lin, D. Y. C. Shih. Isolation and Identification of New Sildenafil Analogues from Dietary Supplements. *J. Food Drug Anal.* **2013**, *21*, 40–49.
[9] L. Kuo-Chih, L. Yi-Chu, L. Yung-Chih, L. Yun-Lian, T. Li-Yao, L. Jer-Huei, L. Chi-Fang. Isolation and Identification of Three Thio-sildenafil Analogues in Dietary Supplements. *J. Food Drug Anal.* **2010**, *18*, 269–278.
[10] X. Ge, L. Li, H. L. Koh, M. Y. Low. Identification of a new sildenafil analogue in a health supplement. *J. Pharm. Biomed. Anal.* **2011**, *56*, 491–496.
[11] H. J. Park, H. K. Jeong, M. I. Chang, M. H. Im, J. Y. Jeong, D. M. Choi, K. Park, M. K. Hong, J. Youm, S. B. Han, D. J. Kim, J. H. Park, S. W. Kwon. Structure determination of new analogues of vardenafil and sildenafil in dietary supplements. *Food Addit. Contam.* **2007**, *24*, 122–129.
[12] J. C. Reepmeyer, J. T. Woodruff. Use of liquid chromatography–mass spectrometry and a chemical cleavage reaction for the structure elucidation of a new sildenafil analogue detected as an adulterant in an herbal dietary supplement. *J. Pharm. Biomed. Anal.* **2007**, *44*, 887–893.
[13] A. Nieto, M. Peschka, F. Borrull, E. Pocurull, R. M. Marcé, T. P. Knepper. Phosphodiesterase type V inhibitors: Occurrence and fate in wastewater and sewage sludge. *Water Res.* **2010**, *44*, 1607–1615.
[14] H. F. Schröder, W. Gebhardt, M. Thevis. Anabolic, doping, and lifestyle drugs, and selected metabolites in wastewater—detection, quantification, and behaviour monitored by high-resolution MS and MSn before and after sewage treatment. *Anal. Bioanal. Chem.* **2010**, *398*, 1207–1229.

[15] R. L. Oulton, T. Kohn, D. M. Cwiertny. Pharmaceuticals and personal care products in effluent matrices: A survey of transformation and removal during wastewater treatment and implications for wastewater management. *J. Environ. Monit.* **2010**, *12*, 1956–1978.
[16] T. E. Doll, F. H. Frimmel. Fate of pharmaceuticals—photodegradation by simulated solar UV-light. *Chemosphere* **2003**, *52*, 1757–1769.
[17] P. Eichhorn, S. Pérez, J. Aceña, P. Gardinali, J. L. Abad, D. Barceló. Identification of phototransformation products of sildenafil (Viagra) and its N-demethylated human metabolite under simulated sunlight. *J. Mass Spectrom.* **2012**, *47*, 701–711.
[18] L. Blok-Tip, B. Zomer, F. Bakker, K. D. Hartog, M. Hamzink, J. ten Hove, M. Vredenbregt, D. de Kaste. Structure elucidation of sildenafil analogues in herbal products. *Food Addit. Contam.* **2004**, *21*, 737–748.
[19] Reepmeyer J. C., D. A. d'Avignon. Structure elucidation of thioketone analogues of sildenafil detected as adulterants in herbal aphrodisiacs. *J. Pharm. Biomed. Anal.* **2009**, *49*, 145–150.
[20] B. J. Venhuis, M. E. Zwaagstra, J. D. J. van den Berg, A. J. H. P. van Riel, H. W. G. Wagenaar, K. van Grootheest, D. M. Barends, D. de Kaste. Illicit erectile dysfunction products in the Netherlands: A decade of trends and a 2007-2010 product update, in: Illegale erectiemiddelen in Nederland: Analyses van producten (2007-2010) en een decennium van trends, Rijksinstituut voor Volksgezondheid en Milieu RIVM, Dutch Customs Laboratory, Royal Dutch Association for the Advancement of Pharmacy.
[21] M. Alp, M. Coşkun, H. Göker. Isolation and identification of a new sildenafil analogue adulterated in energy drink: Propoxyphenyl sildenafil. *J. Pharm. Biomed. Anal.* **2013**, *72*, 155–158.
[22] S. Ma, Y. Xu, M. Shou. Characterization of imatinib metabolites in rat and human liver microsomes: differentiation of hydroxylation from N-oxidation by liquid chromatography/atmospheric pressure chemical ionization mass spectrometry. *Rapid Commun. Mass Spectrom.* **2009**, *23*, 1446–1450.
[23] R. Ramanathan, A. D. Su, N. Alvarez, N. Blumenkrantz, S. K. Chowdhury, K. Alton, J. Patrick. Liquid Chromatography/Mass Spectrometry Methods for Distinguishing N-Oxides from Hydroxylated Compounds. *Anal. Chem.* **2000**, *72*, 1352–1359.
[24] D. Zhong, J. Xing, S. Zhang, L. Sun. Study of the electrospray ionization tandem mass spectrometry of sildenafil derivatives. *Rapid Commun. Mass Spectrom.* **2002**, *16*, 1836–1843.
[25] R. D. Morrison, A. L. Blobaum, F. W. Byers, T. S. Santomango, T. M. Bridges, D. Stec, K. A. Brewer, R. Sanchez-Ponce, M. M. Corlew, R. Rush, A. S. Felts, J. Manka, B. S. Bates, D. F. Venable, A. L. Rodriguez, C. K. Jones, C. M. Niswender, P. J. Conn, C. W. Lindsley, K. A. Emmitte, J. S. Daniels. The Role of Aldehyde Oxidase and Xanthine Oxidase in the Biotransformation of a Novel Negative Allosteric Modulator of Metabotropic Glutamate Receptor Subtype 5. *Drug Metab. Dispos.* **2012**, *40*, 1834–1845.

Supporting information

Additional supporting information may be found in the online version of this article at the publisher's web site.

